GUMICS-3 — A GLOBAL IONOSPHERE-MAGNETOSPHERE COUPLING SIMULATION WITH HIGH IONOSPHERIC RESOLUTION

P. Janhunen

Finnish Meteorological Institute, Geophysical Research
P.O.B. 503, FIN-00101, Helsinki, Finland
phone: +358 9 1929557, fax: +358 9 1929539
email: Pekka.Janhunen@fmi.fi
Also at Swedish Institute of Space Physics, Uppsala Division, 755 91, Uppsala, Sweden

Abstract

The prediction of satellite charging and other harmful effects can not be succesful unless we can model and predict substorms and other kinds of auroral breakups. For this we need a high-resolution global simulation system whose only essential input consists of measured solar-wind data.

GUMICS-3 ("Grand Unified Ionosphere-Magnetosphere Coupling Simulation, version 3") is a simulation system, which integrates a three-dimensional global magnetohydrodynamic (MHD) simulation box with a high-resolution model of ionospheric electrodynamics. We use a hierarchical rectangular grid, which is recursively refined according to a specified density function. The density function is such that the grid resolution is high in the near-Earth region, at the magnetopause and in the tail current sheet, while the solar wind, far tail and lobe regions have a lower resolution. The finite volume method is used in the MHD equations. The ionospheric conductivities depend on the electron precipitation, along with a dayside enhancement due to solar radiation. A model for field-aligned potential drop (current-voltage relationship) can also be defined. The most important difference between GUMICS-3 and other similar programs is the use of a locally varying timestep. In the near-Earth region the Alfven speed is very high, which makes it necessary to use a very small timestep, sometimes less than 10 ms. In conventional simulation methods the same timestep must be used throughout the grid, but in our version of MHD the timestep is locally adaptive. This results in significant reduction (at least one order of magnitude) of computing time, making it possible to use a previously unavailable resolution in the near-Earth region and in the ionosphere without increasing the computer requirements. The grid spacing in the auroral ionospheric is less than 100 km in the supercomputer versions of the model.

We will present the GUMICS-3 model and show some examples of simulated events where solar wind data has been available. Comparisons with observations will be included. The problems of how to translate the MHD and ionospheric variables produced by GUMICS-3 into useful information about high-energy particle fluxes at geostationary orbit and elsewhere will also be briefly discussed.

1. Introduction

Satellite charging and other harmful effects caused by energetic particles in the Earth's plasma environment can be predicted in principle by two different types of methods. First, one can use detailed numerical simulation models, analogous to those used in everyday numerical weather forecasting, which is the subject of this paper. Second, one can use neural networks and other machine learning tools for the prediction of various indices describing the disturbance level (Kp, Dst, etc.) [Lundstedt and Wintoft, 1994, Vassiliadis *et al.*, 1995]. In both cases the most important input is the solar wind. Ignoring spatial inhomogeneities, the solar wind input can be measured by one single satellite suitably positioned on the sunward side of the magnetosphere. The input quantities are the plasma density, temperature, velocity and magnetic field vector (6 variables).

We can not yet be completely sure but there is some hope that the time series of the solar wind as measured by a single satellite is sufficient input for succesfully predicting the large-scale magnetospheric dynamics (space weather), including substorms. Factors which are neglected in this approach are solar wind inhomogeneities [Ma *et al.*, 1991], long–lived (more than a few hours) radiation belt particle populations and changes in ionospheric composition and neutral winds.

If the input time series is measured by a satellite, the time required to do the numerical computation is about one hour at most (this is the time it takes for the solar wind to arrive from the satellite to the magnetosphere). If longer time spans are needed, we must resort to other, indirect, methods to determine the solar wind data.

Global magnetohydrodynamic (MHD) simulation of the Earth's magnetosphere has shown its effective-

ness in giving accurate predictions for the overall geometry of the magnetosphere [Ogino, 1986, Watanabe and Sato, 1990, Tanaka, 1995, Raeder *et al.*, 1995, Fedder *et al.*, 1995, for example]. Thus it is natural to base a magnetospheric simulation on the MHD equations. However, MHD alone is not sufficient: we must model the ionosphere and the ionosphere-magnetosphere coupling. Also, the usual global MHD simulations have typically rather poor resolution in the near-Earth region, resulting an equally poor ionospheric resolution.

There are two problems in the numerical realisation of high (smallest grid spacing less than 100 km in the ionospheric plane) ionospheric resolution. If we model the innermost region of the magnetosphere by a sphere with (e.g.) 3.7 R_E radius, inside which the MHD equations are not solved but the mapping of the electric currents and the electric field takes place, then 100 km ionospheric plane grid spacing maps to about 700 km, about 0.1 R_E, grid cell size at the inner edge of the MHD equations (the $3.7R_E$ shell). The first problem is that we cannot hope to fill the whole magnetosphere, which is at least $150R_E$ in length, with $0.1R_E$ grid cells because that would yield several billion grid cells, which is not something we can afford now or in the near future. Thus the spatial MHD grid must be strongly nonuniform, with dense grid in the near-Earth region and sparse grid in the solar wind and in the far tail. The second problem is that in an explicit time differencing scheme, the timestep Δt must obey the Courant-Friedrichs-Lewy (CFL) condition: the timestep must be everywhere smaller than the fastest MHD wave travel time across the grid cell. In the near-Earth region the fastest wave phase speed is practically speaking equal to the local Alfvén speed $v_A = B/\sqrt{(\mu_0 \rho)}$. Typically v_A in this region is about 20 000 km/s, which gives us a timestep of 0.02 seconds if $0.1R_E$ grid cells are used. Our approach to deal with this problem is to use a locally varying timestep [Janhunen *et al.*, 1996].

2. Simulation model

The overall structure of the simulation is shown in **Figure 1**. We have a large simulation box which covers the whole magnetosphere (except the very far tail region). Magnetohydrodynamic (MHD) equations are used in that box. The initial condition is a magnetic dipole in homogeneous, cold and tenuous plasma, with a mirror dipole on the sunward side [Raeder *et al.*, 1995]. At time $t = 0$ we turn on an incoming solar wind at $X = +32R_E$. X, Y, Z are the geocentric solar magnetospheric (GSM) coordinates, measured in Earth radii R_E, with the X axis towards the Sun and the Z axis northward along the dipole axis (more accurately: the projection of the

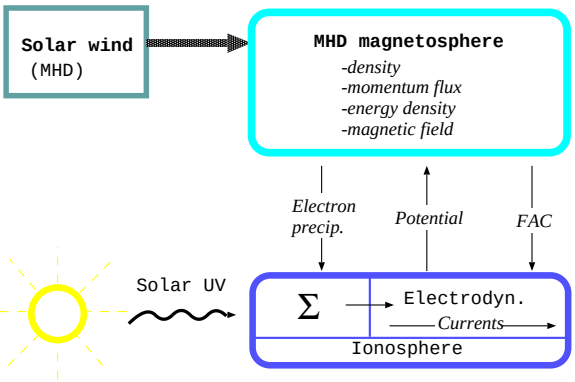

Figure 1: The overall structure of the GUMICS model

dipole axis on a plane perpendicular to X). The Y axis completes the right-handed rectangular coordinate system and points towards eveningside. After about 40 minutes, the basic magnetospheric geometry becomes recognizable: the bow shock, the magnetopause, the magnetosheath, the cusp, the tail current sheet and the plasma sheet become identifiable. For this to happen, only the MHD equations are needed.

The ionosphere is a conducting plane, where the conductivity depends on solar EUV radiation (dayside conductivity enhancement) and on magnetospheric particle precipitation (in this work only electron precipitation is taken into account). The magnetosphere affects the ionosphere in two ways: (1) by giving the electron precipitation which determines the ionospheric conductivity pattern, (2) by giving the field-aligned current (FAC) pattern. The field-aligned current is computed at $3.7R_E$ shell, which is the inner boundary of the MHD equations. The region between the ionosphere and the $3.7R_E$ shell is assumed to be a passive medium which transmits the electric effects between the ionosphere and magnetosphere and where no magnetic field perpendicular currents flow (force-free region). The magnetic field inside $3.7R_E$ radius is assumed to be the dipole field. When the FAC and ionospheric conductivity (actually both Pedersen and Hall conductivity) are known, it is possible to solve the problem of horizontal current distribution in the ionosphere. This can be reduced to solving a 2D elliptic boundary value problem for the electric potential in the ionospheric plane. Once the ionospheric potential is known, we map it to the $3.7R_E$ shell, by also including a parallel electric field contribution (see below). Now that we know the magnetospheric electric potential at the inner edge of the MHD equations, we compute the corresponding $\mathbf{E}\times\mathbf{B}$ velocity, which is finally used as a boundary condition to the MHD equations. This is the only effect that the ionosphere has on

the magnetosphere. The ionosphere/magnetosphere feedback loop is computed every four seconds, but the MHD time stepping is much more frequent.

In this work we write the MHD equations in fully conservative form and expand the magnetic field as $\mathbf{B} = \mathbf{B}_0 + \mathbf{B}_1$, where $\mathbf{B}_0$ is the background dipole field. Below we write the MHD equations without this complication, however, to save space. Otherwise our development follows closely the method of [Tanaka, 1994]: we use a linearized Riemann solution at every cell interface and the Godunov method [LeVeque, 1992]. (We have also programmed the MUSCL method which was used by Tanaka but the results reported in this paper use the Godunov method).

The flux computation routine needs, among other things, the background magnetic field $\mathbf{B}_0$ at the cell interfaces. We found it necessary to compute surface integrals of $\mathbf{B}_0$ over the square shaped cell interfaces. The integrals can be computed analytically for a dipole field. Averaging $\mathbf{B}_0$ over each cell interface ensures that the numerical divergence over every cell is zero within roundoff error. Using pointwise values of $\mathbf{B}_0$ would introduce a spurious $\nabla \cdot \mathbf{B}_0$ of finite magnitude, which would cause serious convergence problems. This point was not explicitly mentioned in Tanaka's papers.

Our earlier program version GUMICS-2 [Janhunen *et al.*, 1996], which also employed a locally varying timestep and hierarchical cubic grid as the current simulation as the present simulation, used a much more primitive spatial differencing scheme (the Lax method). The results were otherwise equal to the present results but contained more smeared profiles of the MHD variables because of higher numerical diffusion. Thus the present simulation (GUMICS-3) is a significant improvement over GUMICS-2.

We now define the model in equation form. The MHD equations are

$$\frac{\partial \rho}{\partial t} = -\nabla \cdot (\rho \mathbf{v}) \,, \tag{1}$$

$$\frac{\partial \mathbf{p}}{\partial t} = -\nabla \cdot \left(\frac{\mathbf{p}\mathbf{p}}{\rho} + P + \frac{B^2}{2\mu_0} - \frac{1}{\mu_0}\mathbf{B}\mathbf{B} \right) \tag{2}$$

$$\frac{\partial u}{\partial t} = -\nabla \cdot \left[(u + P - \frac{B^2}{2\mu_0})\frac{\mathbf{p}}{\rho} + \frac{1}{\mu_0}(\mathbf{B} \times \frac{\mathbf{p}}{\rho} \times \mathbf{B}) \right] , \tag{3}$$

$$\frac{\partial \mathbf{B}}{\partial t} = -\nabla \times \mathbf{E} \tag{4}$$

$$\nabla \cdot \mathbf{B} = 0, \qquad \mathbf{E} + \mathbf{v} \times \mathbf{B} - \frac{1}{en}\mathbf{j} \times \mathbf{B} = 0, \qquad \mathbf{j} \equiv \frac{1}{\mu_\circ} \nabla \times \mathbf{B} \tag{5}$$

$$P \equiv (\gamma - 1) \left(u - \frac{\mathbf{p}^2}{\rho} - \frac{\mathbf{B}^2}{2\mu_0} \right) , \qquad \mathbf{p} \equiv \rho \mathbf{v} \tag{6}$$

At the equation level, the ionospheric model is similar to our earlier works [Janhunen and Huuskonen, 1993, Janhunen *et al.*, 1995, Janhunen *et al.*, 1996]. We have the height-integrated current continuity equation,

$$-\nabla \cdot \left(\Sigma_P \nabla \Phi_i + \Sigma_H \hat{\mathbf{b}} \times \nabla \Phi_i \right) = j_\parallel^{(i)} \sin I, \tag{7}$$

$$\Sigma_{P,H} = \int dh F_{P,H} n \tag{8}$$

where the coefficients $F_{P,H}$ tell how to obtain the local Pedersen (P) and Hall (H) conductivity values from the electron density n. The electron density n is solved in a 3D ionospheric grid using 20 nonuniform levels in height,

$$\frac{\partial n}{\partial t} = q - \alpha n^2 \tag{9}$$

where q is the ionization production caused by magnetospheric processes,

$$q = Q(\chi \rho, T, \Phi_m - \Phi_i), \tag{10}$$

where Q is a precomputed, tabulated function of three arguments: the source plasma density, temperature and the local magnetosphere-ionosphere parallel potential drop. For the definition of χ, see the discussion below. The parallel potential drop is assumed to be related to the field-aligned (parallel) current density by the formula

$$j_\parallel^{(i)} = K(\Phi_m - \Phi_i). \tag{11}$$

Here K is the Lyons-Evans-Lundin "constant", which in the present simulation is computed from

$$K = \frac{\chi n e^2}{\sqrt{2\pi m_e k_B T_e}} \tag{12}$$

according to [Fridman and Lemaire, 1980, equation 12]. The factor χ is the loss cone filling rate, which

is a dimensionless number between 0 and 1. Zero χ means that no new electrons arrive to the loss cone during one electron bounce period and unit χ means that the loss cone is completely filled with thermal electrons during one bounce period (strong pitch angle scattering). In case of zero χ, the field-aligned conductance would be K zero, and the ionization production q would vanish as well. Within MHD equations there is no self-consistent way to compute χ, so we are using an analytic model: Inside the polar cap χ is very close to unity and drops to a small value (0.02) at the equatorward edge of the mean auroral oval. Between these extremes (i.e., within the auroral oval) χ varies smoothly and monotonically. In addition, we include another contribution for χ, which is proportional to $\tau_B(1/T)\max(0, \mathbf{v}\cdot\nabla T)$. Here τ_B is an approximation to the electron bounce period and T is the local MHD plasma temperature. This expression tries to model the adiabatic heating of the particles in regions where plasma convects towards the Earth ($\mathbf{v}\cdot\nabla T > 0$). If χ thus computed becomes larger than one, it is set equal to one.

The locally varying time stepping scheme in the present model is similar to the one described in [Janhunen *et al.*, 1996]. The program has been written in Tela programming language [Janhunen, 1994-1996], except that the MHD solver, which is the most time consuming part, has been written in C++ and linked to Tela. The model is usually run on Cray C90 and achieves 250-300 MFLOPS (million floating point operations per second) performance. The results presented here use about 180 000 grid cells. With this spatial grid the model is usually 3-5 slower than real time (the variability is due to the adaptive, local time stepping). Our spatial grid is of the hierarchical cubic type [Gombosi *et al.*, 1996]. If an equivalent stretched Cartesian grid with global time stepping were used [Raeder *et al.*, 1995], 25 times more computer time would be required, according to our estimation.

3. Results

Figure 2 shows simulated satellite data from GUMICS-3. The satellite is at $(X, Y, Z) = (-10, 0, 0)$, i.e. in the near-Earth magnetotail at midnight meridian and in the equatorial plane. The upper panel shows B_z (the dipole contribution is included). At about $t = 150$ min B_z starts to grow at the satellite position, which is a signature of field dipolarization in the near-Earth region, which is usually associated with substorm expansion phase. Before that, B_z was getting smaller and smaller, which is a typical substorm growth phase signature. The lower panel shows fast (almost 200 km/s) earthward plasma flow associated with the dipolarization. The

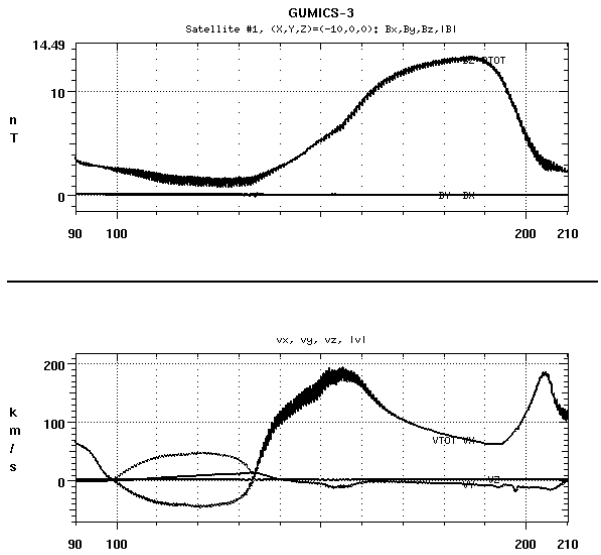

Figure 2: Simulated satellite data for a satellite at $(-10, 0, 0)$. Upper panel shows mainly B_z (B_x,B_y are very small). Lower panel shows the plasma velocity components; only v_x is significant. The time axis is in minutes from the start of the simulation (entry of solar wind).

short variations in the curves are due to MHD wave activity.

4. Discussion and summary

Let us discuss the promises and weaknesses of our model. The model can accept arbitrary solar wind input and a nonzero dipole tilt angle can be used, so the model is ready for application to real events. However, we can anticipate some degradation in the quality of the results for large dipole tilts because the tail current sheet will then move away from the $Z = 0$ plane and thus the densification of the grid is not exactly in the same location where the current sheet forms. This is not a serious problem, however, and can in principle be fixed by redesigning the grid point density function or by going to solution-adaptive grids [Gombosi *et al.*, 1996].

The model produces the overall geometry and current systems of the magnetosphere quite well. On the dayside, the bow shock, the magnetosheat, and the magnetopause can be clearly seen. The boundaries of the cusp are clear in plasma density and pressure (this was used as a measure of goodness of an MHD simulation by *Tanaka* [1994]). The Region-1 current system is always visible and its magnitude depends on the sign of IMF B_z. The closure path of Region-1 current system was studied already by *Janhunen et al.* [1996] using GUMICS-2, who found agreement

with the results of *Tanaka* [1995]. The Region-2 current system is clearly weaker and it vanishes almost totally for northward IMF B_z. With the accuracy of GUMICS-3 we are also able to study the closure path of Region-2 current but we shall not include this study in the current paper. During northward IMF B_z, a current system develops close to the magnetic pole, which is similar to the so-called NBZ current system [Ijima and Shibaji, 1987]. After a period of southward IMF B_z, substorm signatures (dipolarization, fast flows) are seen in the near-Earth magnetotail, together with enhanced Alfvén wave activity bouncing between the ionosphere and the magnetosphere. An auroral brightening is observed in the ionosphere at the same time. A substorm current wedge (SCW) can be identified in the ionosphere and we can trace it to the magnetosphere. However, the total current flowing in the wedge is only about 25 kA in the case simulated, which is insufficient of producing the negative magnetic "bay" in ground magnetograms, which is a typical substorm signature. Thus, although we can list numerous substorm signatures in our simulation, we still cannot say that we are simulating a real substorm because a well–developed SCW does not form. It may be, of course, that just by increasing the IMF variation magnitude we could increase the magnitude of the current wedge. This remains to be seen in future simulation runs.

Maybe the most important weakness of the model, as far as harmful effects of energetic particles are concerned, is the lack of kinetic description of the plasma. The MHD equations do not properly describe situations where the particle populations are far from Maxwellian, neither do they describe pressure and temperature anisotropies. Thus we cannot predict energetic particle fluxes directly but must relate these to the MHD variables (pressure, density, temperature) by some indirect means. Related to the lack of kinetic description is that fact that we cannot compute the loss cone filling rate χ self-consistently but are forced to use an analytic model for it as was described above. This means that we cannot compute the electron precipitation and thus the ionoshperic conductivities fully self-consistently. By changing our χ model we generally get different results. A related problem is also the electron temperature, which is also needed in Knigth's formula for precipitating electron flux: The MHD equations produce only a single plasma temperature (ion plus electron temperature). Experimental results indicate that the electron temperature is often significantly smaller than the ion temperature, but we have no self-consistent way of computing the temperature ratio within the framework of MHD.

Many figures and animations related to this work can be found using WWW at `http://www.geo.fmi.fi/~pjanhune/gumics3/`.

References

Fedder *et al.*, 1995. Fedder, J. A.; Lyon, J. G.; Slinker, S. P.; Mobarry, C. M., Topological structure of the magnetotail as a function of interplanetary magnetic field direction, J. Geophys. Res., 100, 3613–3621, 1995.

Janhunen and Huuskonen, 1993. Janhunen, P. and Huuskonen, A., A numerical ionosphere-magnetosphere coupling model with variable conductivities, J. Geophys. Res., 90, 9519–9530, 1993.

Janhunen *et al.*, 1995. Janhunen, P., Pulkkinen, T.I., and Kauristie, K., Auroral fading in ionosphere-magnetosphere coupling model: Implications for possible mechanisms, Geophys. Res. Lett., 22, 2049–2052, 1995.

Janhunen *et al.*, 1996. Janhunen, P., Koskinen, H.E.J., Pulkkinen, T.I., A new global ionosphere-magnetosphere coupling simulation utilizing locally varying time step, in Proceedings of Third International Conference on Substorms (ICS3), Versailles, France, May 12-17, ESA SP 1996.

Fridman and Lemaire, 1980. Fridman, M. and Lemaire, J., Relationship between auroral electrons (sic) fluxes and field aligned electric potential difference, J. Geophys. Res., 85, 664–670 1980.

Gombosi *et al.*, 1996. Gombosi, T.I., DeZeeuw, D.L., Hberli, R.M. and Powell, K.G., Three-dimensional multiscale MHD model of cometary plasma environments, J. Geophys. Res., 101, 15233–15253, 1996.

Ijima and Shibaji, 1987. Ijima, T. and Shibaji, T., Global characteristics of northward IMF-associated (NBZ) field-aligned currents, J. Geophys. Res., 92, 2408–2424, 1987.

LeVeque, 1992. LeVeque, R.J., Numerical methods for conservation laws, Birkhuser, 1992.

Lundstedt and Wintoft, 1994. Prediction of geomagnetic storms from solar wind data with the use of a neural network, Ann. Geophys., 12, 19–24, 1994.

Ma *et al.*, 1991. Ma, Z.W., Hawkins, J.G., Lee, L.C., A simulation study of impulsive penetration of solar wind irregularities into the magnetosphere at the dayside magnetopause, J. Geophys. Res., 96, 15751–15765, 1991.

Raeder *et al.*, 1995. Raeder, J.; Walker, R. J.; Ashour-Abdalla, M., The structure of the distanct geomagnetic tail during long periods of northward IMF, Geophys. Res. Lett., 22, 349–352, 1995.

Tanaka, 1994. Tanaka, T., Finite volume TVD scheme on an unstructured grid system for three-dimensional MHD simulation of inhomogeneous systems including strong background potential fields, J. Comp. Phys., 111,, 381–389, 1994.

Tanaka, 1995. Tanaka, T., Generation mechanisms for magnetosphere-ionosphere current systems deduced from a three-dimensional MHD simulation of the solar wind-magnetosphere-ionosphere coupling processes, J. Geophys. Res., 100, 12057–12074, 1995.

Janhunen, 1994-1996. Tela the Tensor Languagea: A scientific computing environment, `http://www.geo.fmi.fi/prog/tela.html`, 1994-1996.

Ogino, 1986. Ogino, T., A three-dimensional MHD simulation of the interaction of the solar wind with the earth's magnetosphere - The generation of field-aligned currents, J. Geophys. Res., 91, 6791–6806, 1986.

Vassiliadis *et al.*, 1995. Vassiliadis, D., Klimas, A.J., Baker, D.N., Roberts, D.A., A description of the solar wind-magnetosphere coupling based on nonlinear filters, J. Geophys. Res., 100, 3495–3512, 1995.

Watanabe and Sato, 1990. Watanabe, K. and Sato, T., Global simulation of the solar wind-magnetosphere interaction - The importance of its numerical validity, J. Geophys. Res., 95, 75–88, 1990.